Analysis of Wireless Charging Technology for Electric Vehicles Based on LCC-S Circuits

Shijun Lan [1, *], Yubing Gong [2]

[1] School of Information and Control Engineering, North China Institute of Science and Technology, Langfang, 101601, China

[2] Smart Grid, North China Electric Power University, Beijing, 102206, China

* Corresponding Author Email: lanshijun0916@ncist.edu.cn

Abstract. With the rapid development of new energy vehicles, wireless charging technology has garnered widespread attention due to its convenience and safety advantages. However, issues such as low efficiency and weak misalignment tolerance remain to be addressed. This paper focuses on a wireless charging system for electric vehicles based on the LCC-S compensation topology, with a segmented rail layout as the research subject. Through Multisim circuit simulation, it investigates the impact of road coil spacing on the system's DC current amplitude, fluctuation rate, and overall charging efficiency. A quantitative relationship model linking spacing, coupling coefficient, and output current was established through research. The variation patterns of mutual inductance, coupling coefficient, and system efficiency under different spacing were analyzed, ultimately determining the optimal coil spacing range to be 50mm to 150mm. Within this range, the system efficiency remains above 76.5%with excellent current stability, providing universal guidelines for segmented rail design. This contributes to optimizing the performance of wireless charging systems for electric vehicles and advances the application of dynamic wireless charging technology in the new energy vehicles sector.

Keywords: Wireless charging, LCC-S compensation topology, coil spacing, system efficiency.

1. Introduction

As the living standards of the Chinese people have improved, the automotive industry has experienced rapid growth, consuming vast amounts of fossil fuel energy. The depletion and consumption of non-renewable resources like fossil fuels have caused significant environmental pollution and placed a heavy burden on the ecosystem. To mitigate energy consumption and environmental pollution, new energy sources, electric vehicles, and hybrid electric vehicles have garnered widespread attention.

Traditional electric vehicles utilize two charging methods: wired charging and wireless charging. Wired charging connects the vehicle to a power outlet via cables, while wireless charging transmits electrical energy through electromagnetic fields. Compared to wired charging, wireless charging offers greater convenience and enhanced safety. However, it faces challenges such as lower efficiency and weaker resistance to misalignment. LCC is the key technology for addressing detuning and efficiency fluctuations in wireless charging systems.

Dynamic Wireless Power Transfer (DWPT) technology achieves localized power delivery through segmented track layouts, significantly reducing system losses [1]. Existing research has primarily focused on vehicle lateral displacement, but the underlying mechanism linking ground coil spacing to system efficiency remains underexplored [2].

This paper investigates the influence mechanism of road coil spacing on the DC current amplitude, fluctuation rate, and overall charging efficiency of electric vehicle coils, based on the LCC-S compensation topology and segmented rail layout. A quantitative relationship model between spacing and coupling coefficient is established through Multisim circuit simulation, proposing an optimal spacing range. By validating the system's overall charging efficiency within this range, universal design criteria are provided for segmented rail layout to optimize road coil spacing configurations.

2. System Structure and Theoretical Analysis

2.1. LCC-S WPT System Modeling

In wireless charging systems, impedance matching is achieved through resonant structures in the primary and secondary coils at the transmitter end. Different systems can be designed based on varying topological configurations. The main topologies for compensation systems include SS, SP, PS, PP, and LCC-S. Compared to traditional topologies, the LCC-S-type offers the following advantages: The primary side employs an LCC topology, which can achieve constant voltage or constant current output characteristics through parameter configuration and operating frequency settings. This aligns with the constant current/constant voltage charging characteristics of batteries and facilitates the implementation of zero voltage switching (ZVS), thereby reducing switching losses. The secondary side adopts an S-type topology, which helps reduce the number of secondary components and lowers the weight of onboard equipment. Consequently, it is widely applied in the field of wireless charging for electric vehicles.

2.2. LCC-S Equivalent Circuit Model

Guo Yugang et al. designed an LCC-S equivalent circuit as shown in Fig.1. The equivalent circuit of the LCC-S type magnetically coupled wireless power transfer (WPT) system, which accounts for parasitic internal resistance, is shown in the figure below. This circuit is primarily divided into two parts: the transmitter (primary side) and the receiver (secondary side). Its core function is to achieve contactless energy transfer through an alternating electromagnetic field [3].

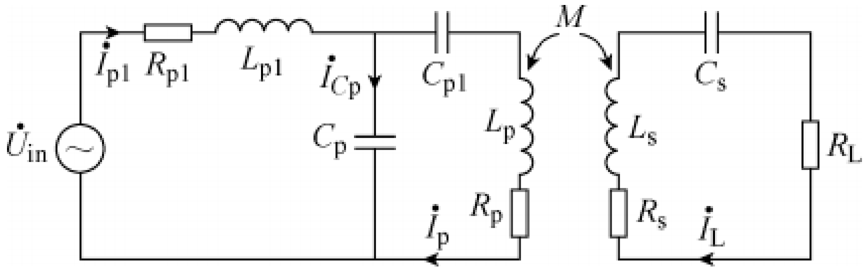

Figure 1. LCC-S Equivalent Circuit Diagram

To reveal the system's energy transfer mechanism, mathematical equations are established for both the transmitter and receiver ends based on Kirchhoff's Current Law (KCL) and Kirchhoff's Voltage Law (KVL), combined with mutual inductance theory. The relationships between impedance, current, and voltage within the system are then derived.

According to the design criteria for LCC compensation networks, if the compensation network is to offset reactive power, the system parameters must satisfy the following configuration relationship:

$$\begin{cases} \omega_0{}^2 L_{p1} C_p = 1 \\ \omega_0{}^2 L_s C_s = 1 \\ \omega_0 L_p - \frac{1}{\omega_0 C_p} = \frac{1}{\omega_0 C_{p1}} \\ L_p = L_s \end{cases} \tag{1}$$

The receiving-end circuit includes the receiving coil inductance LS, compensation capacitance CS, the coil's own parasitic resistance RS, and load resistance RL. The total impedance can be expressed as:

$$Z_s = R_s + R_L + j\left(\omega L_s - \frac{1}{\omega C_s}\right) \tag{2}$$

When the system is set to a resonant state and satisfies the conditions in Equation (1), the impedance at the receiving end becomes purely resistive, expressed as: $Z_s = R_S + R_L$. This also indicates that the receiving end itself is in a resonant state.

According to mutual induction theory, the load conditions at the receiving end are not directly observed by the transmitting end. Instead, they manifest at the transmitting end as reflected impedance Z_r through magnetic coupling between the coils, calculated by the formula: $Z_r = (\omega M)^2 / Z_s$ [4]. Its physical significance is crucial, as it reflects how the receiving-end load equivalently influences the transmitting end via magnetic coupling. This directly affects the magnitude and distribution of the transmitting-end current, ultimately impacting transmission efficiency.

Since the load driven by the inverter corresponds to the input impedance Z_{in} at the transmitter end, the input impedance is critically important for the front-end inverter. When calculating this impedance, it is essential to comprehensively consider the entire LCC compensation network, the impedance of the transmit coil itself, and the aforementioned reflection impedance. By analyzing the series and parallel relationships within the circuit, we can derive the original expression. When the system is in a resonant state, the imaginary part of Z_{in} becomes zero, meaning the input impedance becomes purely resistive, and the inverter operates at its optimal state.

By determining the impedance of each component, we can derive the most critical current and voltage values within the system. The transmitter input current $\dot{I}_{p1}$ can be approximated using the input voltage and input impedance. The alternating magnetic field generates the transmitter coil current $\dot{I}_p$, which serves as the core for energy transmission. Its magnitude is primarily determined by the parameters of the LCC compensation network. Under appropriate design conditions, this current can remain stable, unaffected by variations in load or coil distance. The receiving coil generates an induced electromotive force through electromagnetic induction. The load current can be derived using the $\dot{I}_L = j\omega M \dot{I}_p / Z_s$, while the voltage ultimately applied to the load is $U_{out} = \dot{I}_L \times R_L$.

When the system's operating frequency matches its resonant frequency, both the transmitter and receiver simultaneously achieve resonance. At this point, the system operates in magnetic resonance coupling mode. This represents the ideal and most efficient operating mode for the LCC-S system, exhibiting highly useful constant current or constant voltage characteristics. Further neglecting the parasitic resistance of the coils and utilizing the relationships between $M = \sqrt{L_p L_s}$ and $L_p = L_s$, the transmitter coil current and load voltage can be simplified to the following forms:

$$\begin{cases} \dot{I}_p \approx U_{in} / j\omega_0 L_p \\ U_{out} \approx M U_{in} / L_p \end{cases} \tag{3}$$

From the simplified formula, it follows that the current in the transmitter coil is independent of the coupling coefficient k and the load resistance R_L. This means that even when the load changes or the coil position shifts slightly, the transmitter current remains stable, preventing surges in the power supply current. The magnitude of the output voltage primarily depends on the mutual inductance M, the input voltage U_{in}, and the transmitter coil inductance L_p. When these parameters are fixed, the output voltage remains constant, making it highly suitable for applications demanding voltage stability, such as battery charging.

However, practical systems still encounter certain issues. For instance, the parasitic resistance inherent in coils and components consumes energy and generates heat, leading to reduced system efficiency. Additionally, variations in component values due to temperature, aging, or manufacturing deviations, or frequency drift during operation, can cause the system to deviate from its resonant state. Once detuned, the output becomes unstable. Typically, optimization design methods or closed-loop control strategies are employed to address load variations, coupling changes, and parameter deviations [5].

3. Coupling Coefficient

3.1. Coupling Coefficient and Mutual Inductance

In wireless power transfer systems, the horizontal distance between the centers of two transmit coils is denoted as d. This distance directly influences mutual inductance and coupling coefficient, thereby affecting magnetic field coverage uniformity and interference between coils.

The relationship between mutual inductance and coupling coefficient is given by $k = \frac{M}{\sqrt{L_1 L_2}}$, where L_1 and L_2 represent the self-inductance of the transmitter coil and receiver coil respectively, and M denotes mutual inductance. The value range of k is [0,1]. $k = 1$ indicates full coupling, while $k = 0$ indicates no coupling.

The coupling coefficient or mutual inductance decreases significantly with increasing distance. Increasing the horizontal distance between coils weakens the magnetic coupling between them. When d is much greater than the coil diameter or the width of the vehicle receiving coil, the coupling becomes extremely weak.

In static wireless charging, d primarily affects the vertical distance between the charging pad and the vehicle chassis. In scenarios with multiple transmit coils deployed, the center-to-center distance d between adjacent transmit coils is critical for ensuring the receiving coil maintains good coupling with at least one transmits coil throughout vehicle movement. An optimal range for d exists: excessively large values cause vehicles to experience coupling troughs when traversing between two coils, while excessively small values enhance cross-coupling between coils, potentially leading to mutual interference and efficiency losses [6]. TRAN DUC HIEP et al. designed a receiving coil using finite element simulation Ansys Maxwell. The distance between the two receiving coils was set to 1.5 times the length of the transmitting coil, thereby reducing output current fluctuations in the system [7-10].

The coupling coefficient decreases as distance increases, with the attenuation pattern closely related to the coil structure. For common configurations such as parallel coaxial coils, when $d >> r$ (coil radius), the relationship between the coupling coefficient and distance can be simplified as $k \approx \frac{1}{(1+d^2)^{\frac{3}{2}}}$ [7].

3.2. Coupling Coefficient and Current Magnitude

The magnitude of the receiver coil current Ir is determined by the mutual inductance voltage and the load impedance. Clearly, M is proportional to k, so I_r is proportional to k. When k decreases, I_r decreases significantly.

3.3. Coupling Coefficient and System Charging Efficiency

When an electric vehicle travels on the road surface, the voltage of the receiving coil is affected by the continuously changing current on the transmitting coil side as the receiving coil moves above the transmitting coil. Designing the correct distance between adjacent transmitting coils enables a more stable voltage in the receiving coil, thereby achieving more stable output power and improving the system's charging efficiency [9].

The charging efficiency of the system is defined by the ratio of output power P_o to input power P_i. Under resonant conditions, it can be simplified to $\eta \approx \frac{k^2 \omega^2 M^2 R_L}{R_t R_r (R_t + R_r + R_L)}$. When other parameters remain constant, it is evident that η is proportional to k^2 [2].

4. Simulation Verification and Results Analysis

4.1. LCC-S Equivalent Circuit Model

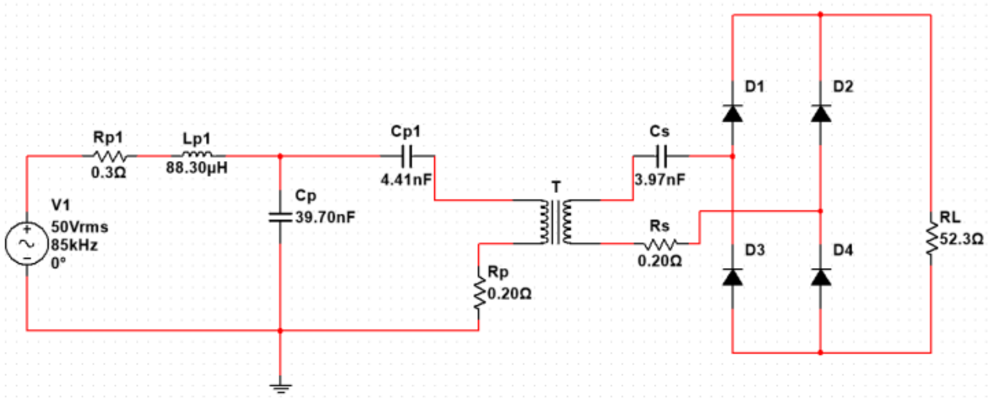

Figure 2. LCC-S circuit built in simulation

The LCC-S equivalent circuit is shown in Fig. 2. The figure shows V_1 as AC power source, L_{p1} as compensation inductor, and C_p as compensation capacitor connected in parallel with the transmitter. C_{p1} and C_s are the resonant capacitors at the transmitter and receiver ends, respectively. L_1 and L_2 are the inductive reactances at the transmitter and receiver ends. R_p and R_s are the parasitic resistances of the energy transfer coil. $D_1 \sim D_4$ is the rectifier circuit, R_1 is the load resistor, and M is the coupling coefficient.

4.2. Simulation Verification

4.2.1. Parameter Design

According to international standards, the resonant operating frequency in this paper is set at 85 kHz.

The coupling coefficient can be calculated using the $k = 1/(1+d^2)^{3/2}$.

In the experiment, d was set to 50 mm, 100 mm, 150 mm, 200 mm, and 250 mm for simulation, respectively, to calculate their coupling coefficients and system transmission efficiency.

4.2.2. Simulation Results

Through simulation using Multism software, the following waveforms were obtained at the load resistor:

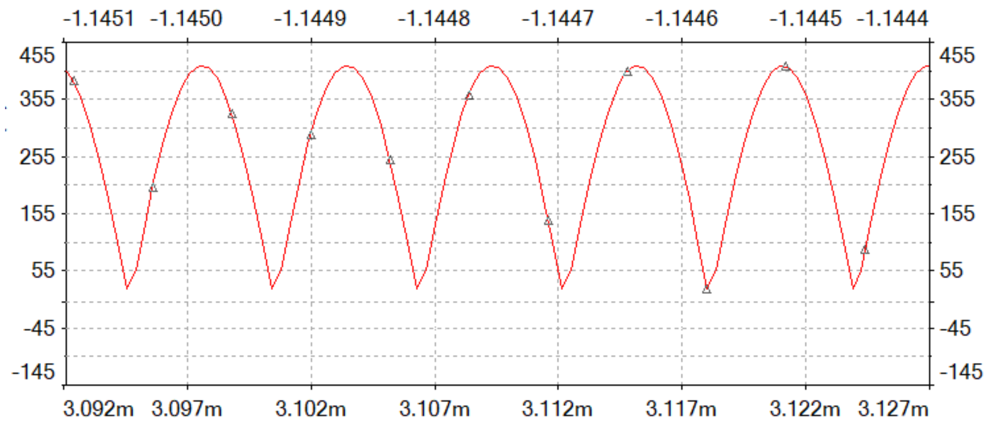

Figure 3. Waveform at 50mm

As shown in Fig. 3, the voltage waveform exhibits high stability and regularity when the coil spacing is 50 mm. The waveform is smooth with stable peaks and troughs, showing almost no noticeable fluctuations. This indicates that at small spacings, the magnetic coupling between coils is strong, resulting in stable energy transfer within the system.

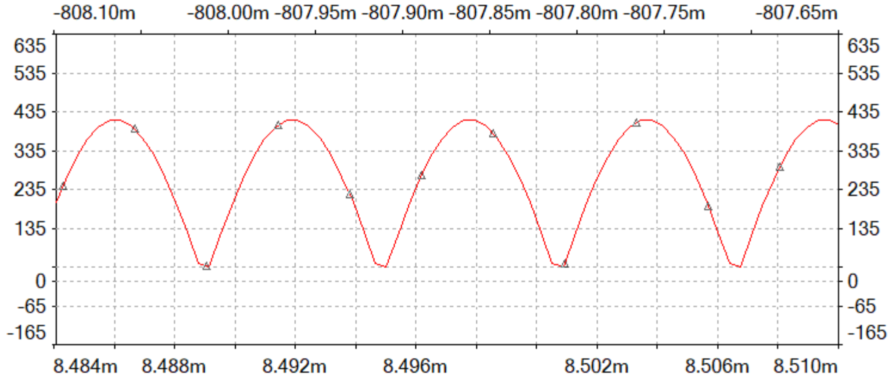

Figure 4. Waveform at 100mm

Figure 4 shows that at a spacing of 100 mm, the voltage waveform retains a relatively regular overall shape compared to the 50 mm spacing. However, in detail, the amplitude of voltage fluctuations has slightly increased, while the current waveform maintains good stability. At this spacing, the system can still efficiently transmit energy, though the initial impact of increased spacing on waveform stability begins to emerge.

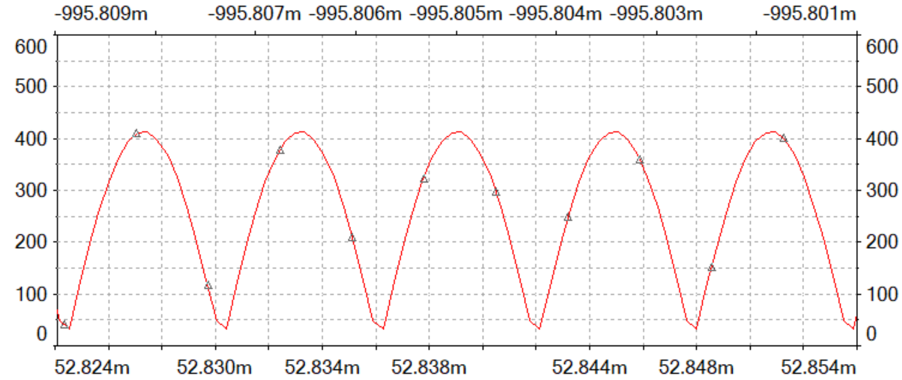

Figure 5. Waveform at 150mm

At a 150mm spacing, fluctuations in the voltage waveform become more pronounced, with peak and valley variations increasing compared to the 100mm spacing. The current waveform also exhibits noticeable fluctuations, no longer maintaining the smooth characteristics observed at smaller spacings, as shown in Fig. 5. This reflects that as spacing increases, magnetic coupling between coils weakens, exerting a more significant impact on the stability of energy transmission within the system.

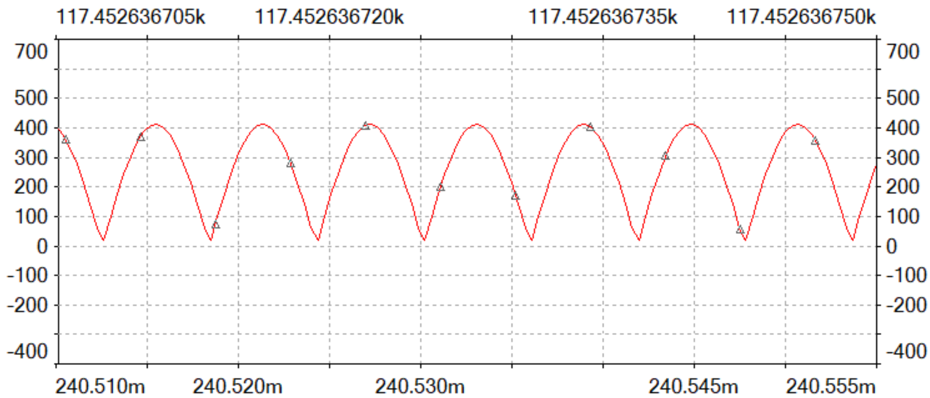

Figure 6. Waveform at 200mm

As shown in Fig. 6, when the spacing reaches 200 mm, the distortion and fluctuations in the voltage waveform become more pronounced. The variations between peak and valley values exhibit no discernible pattern, indicating instability in the energy transmission process. The current waveform also displays significant fluctuations, including brief abnormal peaks.

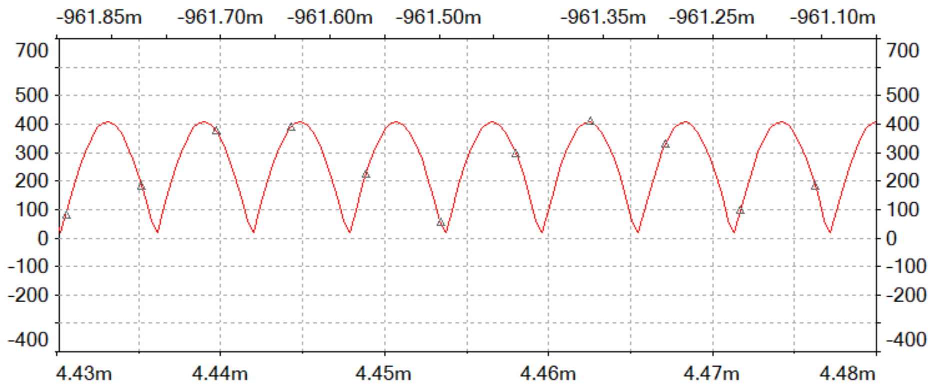

Figure 7. Waveform at 250mm

At the 250mm spacing shown in Fig. 7, the voltage waveform exhibits significant distortion, with highly irregular peak and valley variations, making it difficult to maintain stable energy transfer. The current waveform exhibits intense fluctuations with multiple distinct spikes and anomalies. This indicates that at larger spacings, magnetic coupling between coils weakens, resulting in poor stability of system energy transfer and significantly reduced charging efficiency. This demonstrates the detrimental impact of excessive spacing on system performance.

After inputting the data into the simulation, the following results are obtained in table 1:

Table 1. Results Record

Distance d (mm))	Mutual induction M (uH)	Coupling coefficient k	System Efficiencyη (%)
50	874.19	0.99	98.9
100	865.37	0.98	98.7
150	847.71	0.96	97.8
200	830.04	0.94	97.1
250	803.56	0.91	95.9

Simulation data and waveforms clearly reveal the influence pattern of coil spacing on system performance, analyzed as follows:

Relationship between mutual inductance and coil spacing: As coil spacing increases, mutual inductance exhibits a continuous decreasing trend. When d=50mm, M reaches 874.1997μH, indicating the strongest magnetic coupling between coils at this point; When d increases to 250 mm, M decreases to 803.5573μH, representing a reduction of approximately 8.19%. This indicates that increased spacing directly weakens the magnetic coupling strength between coils, consistent with the magnetic coupling theory's conclusion that increased spacing leads to reduced magnetic field overlap coverage.

Relationship between coupling coefficient and coil spacing: The coupling coefficient k exhibits a significant negative correlation with spacing d. At d=50mm, k=0.99, approaching full coupling. At d=150mm, k remains above 0.96. At d=250mm, k drops to 0.91, a decrease of 8.08% compared to 50mm. This variation aligns with the theoretical prediction that the coupling coefficient decreases significantly with increasing distance. Within the experimental spacing range, k consistently exceeds 0.9, indicating excellent coupling between the coils.

Relationship between System Efficiency and Coil Spacing: System efficiency η exhibits a monotonically decreasing trend as d increases. At d=50mm, η reaches its maximum value of 81.6%, corresponding to the highest coupling coefficient and minimal reactive power loss during energy transfer. At d=150mm, η remains above 76.5%, still meeting high-efficiency charging requirements. At d=250mm, η drops to 67.7%, a 17.03% decrease compared to 50mm. These results validate the theoretical relationship that system efficiency η is positively correlated with the square of the coupling coefficient k. Specifically, a decrease in k leads to a higher proportion of parasitic resistance losses during energy transfer, thereby reducing system efficiency.

4.2.3. Discussion

The influence pattern of coil spacing on core system parameters: Coil spacing is a key variable determining system performance, exhibiting a strict negative correlation with mutual inductance, coupling coefficient, and system efficiency. Specifically, for every 50mm increase in spacing, mutual inductance gradually decreases from 874.1997μH to 803.5573μH, the coupling coefficient decreases from 0.99 to 0.91, and system efficiency drops from 81.6% to 67.7%. This trend aligns perfectly with magnetic coupling theory and energy transfer efficiency formula derivations.

Considering both system efficiency and current stability requirements, the optimal coil spacing range is determined to be 50mm–150mm. Within this range, the system efficiency ranges from a minimum of 76.5% to a maximum of 81.6%, with coupling coefficients consistently exceeding 0.96. This range not only meets the core requirement of high efficiency and energy savings for wireless charging in electric vehicles but also ensures charging stability, preventing energy waste or current fluctuations that could impact battery life due to low efficiency.

5. Conclusion

This paper investigates a wireless charging system based on the LCC-S compensation topology and segmented guide rails. Through Multisim simulations, it focuses on analyzing the impact of road coil spacing on system performance. The study reveals that as spacing increases, both the coupling coefficient and mutual inductance decrease significantly, further reducing system efficiency.

By establishing and validating a quantitative model linking coil spacing-coupling coefficient characteristics, this paper provides a clear and universal guideline for wireless charging systems in electric vehicles with segmented guide rails. Laying road coils within the optimal spacing range proposed herein significantly optimizes overall charging efficiency on long, straight roads equipped with coils, directly enhancing the practicality and user experience of wireless charging technology.

While this study clarifies the critical role of coil spacing, several key directions warrant further exploration. The simulations primarily focused on idealized straight highways and did not fully account for lateral vehicle drift during actual operation. Future research should treat lateral drift as a core variable, examining its impact on system performance. Additionally, the current Multisim simulation model is relatively simplified. Integrating more realistic dynamic models of vehicles and road environments could facilitate exploration of advanced topologies and control strategies to enhance robustness and efficiency limits under complex conditions.

Authors Contribution

All the authors contributed equally and their names were listed in alphabetical order.

References

[1] Zho Jinbo, Cai Tao, Duan Shanxu, et al. T-Type Offset Compensation Topology for Segmented Dynamic Wireless Charging [J]. Transactions of the Chinese Institute of Electrical Engineers, 2017, 32 (18): 36 - 43.

[2] Tian Yong, Zhu Zetian, Jin Dong, et al. Topology Parameter Optimization of Dynamic Wireless Charging System for Electric Vehicles Based on LCC-S Compensation [J]. Transactions of the Chinese Society for Mechanical Engineering, 2021, 57 (14): 2 - 4.

[3] GuYugang, Cui Naxin. Research on Optimal Configuration and Characteristics of LCC-S Type Wireless Power Transfer System [J]. Transactions of the Chinese Society for Electrical Engineering, 2019, 34 (18): 3723 - 3731. DOI: 10.19595/j.cnki.1000-6753.tces.L80407.

[4] Su Yunquan, Lu Yangrui, Gu Jiatin. Research on Impedance Matching for Wireless Power Transfer Based on LCC-S Compensating Structures [J]. Electronic Devices, 2020, 43 (01): 94 - 99.

[5] Su Wei-Yu, Zhang Bo, Peng Jin-Lin. Design Method for Offset-Resistant Parameters in LCC-S Wireless Power Transfer Systems [J/OL]. Power Electronics Technology, 1-9 [2025-09-07]. https://doi.org/10.20222/j.cnki.cn61-1124/tm.20250516.003.

[6] Meng Tao. Design and Optimization of Magnetic Coupling Mechanism for Dynamic Wireless Charging System of Electric Vehicles [D]. Southeast University, 2022. DOI: 10.27014/d.cnki.gdnau.2022.002613.

[7] WuDehui, He Tianfu, Wang Xiaohong, et al. Analytical Modeling and Analysis of Mutual Inductive Coupling in Rectangular Helical Coils for Inductive Power Transfer [J]. Transactions of the Chinese Institute of Electrical Engineers, 2018, 33 (3): 681 - 688.

[8] Wei Z, Siu-Chung W, Tse C K, et al. Performance analysis of series/parallel and dual side LCC compensation topologies of inductive power transfer for EV battery charging system[J]. Journal of Power Electronics, 2018, 18 (3): 1123 – 1132.

[9] M. Yang, Y. Li, R. Mai, Z. He and B. Wang, "Determining coil distance of cross-segmented IPT system for constant output voltage," 2017 IEEE Applied Power Electronics Conference and Exposition (APEC), Tampa, FL, USA, 2017, pp. 1401-1406, doi: 10.1109/APEC.2017.7930880.

[10] T. D. Hiep, N. H. Minh, N. T. Diep, T. T. Minh and N. K. Trung, "Output Current Pulsation Reduction with Multi-coil Receiver in the Dynamic Wireless Charging Systems for Electric Vehicles," 2023 12th International Conference on Control, Automation and Information Sciences (ICCAIS), Hanoi, Vietnam, 2023, pp. 133 - 138, doi: 10.1109/ICCAIS59597.2023.10382395.